Research papers

Flow Measurement and Instrumentation

Bed-mounted Electro Magnetic meters: Assessment of the (missing) technical parameters

Damjan Ivetić, Dušan Prodanović, Luka Stojadinović, Dragutin Pavlović

DOI: https://doi.org/10.1016/j.flowmeasinst.2019.101588

Bed-mounted Electro Magnetic meters: Assessment of the (Missing) Technical Parameters

Damjan Ivetić [1], Dusan Prodanović [2], Luka Stojadinović [3], Dragutin Pavlović [4]

[1] PhD Student, University of Belgrade, Faculty of Civ. Eng., Bul. kralja Aleksandra 73, Belgrade 11000, Serbia, (corresponding author) e-mail: *divetic@grf.bg.ac.rs*
[2] Professor, University of Belgrade, Faculty of Civ. Eng., Bul. kralja Aleksandra 73, Belgrade 11000, Serbia
[3] Researcher, Jaroslav Černi Water Institute, Jaroslava Černog 80, 11226 Belgrade, Serbia
[4] Assistant Professor, University of Belgrade, Faculty of Civ. Eng., Bul. kralja Aleksandra 73, Belgrade 11000, Serbia

ABSTRACT

Flow measurements in Urban Drainage Systems (UDS) are essential for pollution control and system management. Since the accuracy of, today the most popular, Acoustic Doppler Velocimeters is impeded by several factors, this research is focused on the alternative, or a supplemental, Electro-Magnetic Velocity (EMV) meters. EMV meters are more robust and can provide accurate low flow measurements, even when covered with porous sediment. However, the downside of EMV is the small control volume (CV) where the flow velocities are integrated in a non-linear manner to obtain a single, one-dimensional measured velocity. For a better understanding of the sensor output and measured mean flow velocity with quantified uncertainty, it is necessary to determine the size of the CV and to understand the non-linear integration principle within the CV. Valuable technical parameters, needed for describing these EMV properties, are typically not provided by the manufacturers. Fundamentally, they could be defined with the magnetic field and "virtual" current distributions. To allow for a more practical interpretation of the EMV operating principle, a simplified model of an EMV sensor is proposed here. The suggested model describes the EMV operating principle with only two technical parameters, one-dimensional weighting function w and the reach of the CV, the τ_{max}. Furthermore, a methodology is proposed for defining these two parameters, using two lab flume experiments. The first one is focused on the investigation of the EMV output, when the EMV is covered by the porous sediment with different depths. The second experiment involves the determination of the longitudinal velocity distribution within the lab flume and the CV of the EMV meter. A backward analysis is suggested to formulate a minimization problem, from which the unknown technical parameters are assessed. The proposed procedure was applied on the examined Flat DC-2 EMV meter. Derived one-dimensional weighting function w exponentially drops with the distance from the electrodes, while the reach of the CV was found to be τ_{max} = 8.7 cm. These parameters, and the simplified model, were validated against the EMV outputs acquired in the lab flume, without sediment presence.

Keywords:

Velocity measurements, Electro Magnetic Velocity meters, Urban Drainage Systems, Weighting function, Control Volume, Laboratory test

List of Abbreviations

ADV	Acoustic Doppler Velocimeters
CFD	Computational Fluid Dynamics
CFM	Correction Function Model

CV	Control Volume
CVP	Central Vertical Profile
EM	Electro-Magnetic
EMF	Electro-Magnetic Flowmeter
EMV	Electro-Magnetic Velocity (meter/sensor)
GUM	Guide to the expression of Uncertainty in Measurement
RMSE	Root Mean Square Error
SME	Small and Medium Enterprise
SNR	Signal to Noise Ratio
UDS	Urban Drainage Systems
VA	Velocity – Area

List of Symbols

$A(h)$, A	Cross–sectional area [m^2]
Ar	The aspect ratio between the flume width B and channel depth h [/]
$\boldsymbol{\alpha}$	The row ($1 \times N$) vector of correction function slopes [/]
α_m	Correction function slope for the m-th experiment run [/]
$\vec{B}$	Magnetic induction [T]
β_m	Correction function intercept for the m-th experiment run [/]
C_{Ar}	Aspect ratio parameter [/]
δ	Sediment depth [m]
δ_m	Sediment depth in the m-th experiment run [m]
E	The induced voltage between the electrodes [V]
H	Sensor height [m]
h	Water depth [m]
h_B	Benchmark water depth measurement [m]
i	Discretization node number
$\vec{j}$	Virtual current vector [A/m^2]
k_s	Roughness height [mm]
κ	Von-Karman constant [/]
L	Sensor length [m]
m	Experiment run number in the experiments with sediment cover
M	Number of experiment runs in the experiments with sediment cover
N	Number of discretization nodes
Q	Flow rate [m^3/s]
Q_f	Flow rate in the parts of CV occupied with the sediment [m^3/s]
$\sin(\theta)$	Energy slope
τ	Control volume [m^3]
τ_{max}	Control volume reach [m]
$u(V)_b$, $u(V)_{b,adj}$	Bias, adjusted bias uncertainty [m/s]
$u(V)_B$	Benchmark uncertainty [m/s]
u_*	Shear velocity [m/s]
V	Mean flow velocity [m/s]
$\vec{V}$	Streamwise velocity field [m/s]
$\mathbf{V}$	The square ($N \times N$) matrix of longitudinal velocity profiles [m/s]

V_0	Measured velocity for $\alpha = 1$ [m/s]
$\overline{V_{B,m}}$	Mean of the 4 benchmark velocity measurements for sediment depth δ_m [m/s]
$\overline{V_{EMV,m}}$	Mean of the 4 EMV velocity measurements for sediment depth δ_m [m/s]
V_{meas}	Measured velocity [m/s]
$V_{S,meas}$	Simulated measured velocity [m/s]
V_x, $V_x(z)$	Longitudinal velocity distribution [m/s]
$\overline{v_x}$	Despiked and averaged ADV longitudinal velocity measurements [m/s]
W	Sensor width [m]
w, $w(z)$	Weighting function [/]
$\overrightarrow{W}$	Weighting vector [/]
$\mathbf{w}$	Weighting function - row ($1 \times N$) vector of coefficients [/]
Z_L	The vertical position of the lower limit of integration [m]
Z_{surf}	The vertical position of the surface of the EMV electrodes [m]
Z_U	The vertical position of the upper limit of integration [m]
z_0	Roughness length of the surface [m]
ξ	Relative position of the boundary between the inner and outer region [/]
ξ_i	Relative distance from the bottom [/]
ξ_{dip}	Value of dip phenomenon [m]

INTRODUCTION

Flow measurements in Urban Drainage Systems (UDS) present a challenging task. Measuring devices have to be designed to operate with partially filled pipes, with varying water depths and a large range of velocities, in environmental conditions commonly characterized as hostile. The selection of the optimal measuring method is governed by hydraulic, physical and environmental conditions along with the properties of the flowing fluid (Godley, 2002). In UDS particularly, the Velocity-Area (VA) method is frequently used. Wet cross-sectional area A can be easily obtained via depth h measurements and known $A(h)$ relation, but the assessment of the mean flow velocity V is a more complex task, since none of the available devices can measure it directly. To obtain the mean flow velocity, it is necessary to find the relationship connecting some measured velocity V_{meas} with the actual mean flow velocity V. This relationship depends on both the used measuring method and the hydrodynamic features of the measuring site (Larrarte 2006, Bonakdari and Zinatizadeh, 2011). As each velocity measuring method is governed by certain technical parameters (Larrarte et al., 2008), for adequate implementation of the VA method in UDS, it is essential to know these parameters of the used sensors.

Commonly in the UDS, velocity measurements are performed with a bed-mounted Acoustic Doppler Velocimeters (ADV) (Larrarte et al., 2008). However, it was shown (McIntyre & Marshall, 2008) that the ability of the ADV to provide accurate velocity measurements in UDS can be impeded by several factors (Maheepala et al., 2001; Aguilar et al., 2016): low flow depths, low velocities, sedimentation, etc. Hence an investigation on alternative, or a supplement method is needed, in order to increase the reliability of flow measurements in UDS. In this paper, the flat bed-mounted Electro Magnetic Velocity (EMV) meter/sensor is analyzed (Svet instrumenata, 2018).

Due to the nature of the operating principle, the EMV meters are potentially more robust and reliable when compared to the ADV. It was shown that EMV meters can provide measurements of the flow velocity even covered by few centimeters of porous sediment (Ivetić et al., 2018a). Additionally, EMV meters have good performance for flows with low depths (smaller than 5 cm) and low, or even reverse velocities (below few cm/s), found in pipes under the back-water effect. These characteristics are particularly valuable in the combined sewer systems where a dramatic difference is observed between dry and wet weather flows (Harremoës et al., 1993). However, the downside of the EMV meters is the small control volume (CV, flow volume contributing to the sensor's output signal) close to the sensor. The velocity measurements are more "local", when compared to the bed-mounted ADV and confined to the parts of the flow near the wall, where the velocity gradients are high. Furthermore, velocity measurements made by the EMV are the result of non-linear integration of flow velocities within the CV (Shercliff, 1962). Therefore, additional care should be taken when defining the relationship between V_{meas} and the actual V. The standard calibration procedure (ISO3455, 2007), performed by the manufacturer is not covering these issues. This relationship should be assessed for the range of flows and hydraulic conditions, through the discharge assessment, or transiting, for given local geometric configuration (El Bahlouli & Larrarte, 2018; Ivetić et al., 2018b). Using numerical modelling of the velocity fields, the observed velocity can be simulated $V_{S,meas}$ and correlated to the V, presuming that the sensor arrangement and technical parameters (describing the measurement principle) are known. Furthermore, the associated uncertainties can be assessed leading to the optimization of the number and position of the sensors. As the manufacturers of EMV meters are typically not providing the user with these technical parameters, a suitable methodology for their derivation is needed. In the literature, such a procedure for the bed-mounted EMVs does not exist.

In this paper, a simplified mathematical model of the bed-mounted EMV is suggested, describing the operating principle of the sensor with two technical parameters, one-dimensional weighting function w and the reach of the CV, the τ_{max}. It is estimated that for practical purposes these two parameters are sufficient to describe the non-linear integrating principle of the EMV meter, needed for establishing the relationship between the measured velocity V_{meas} and the actual mean flow velocity V. Furthermore, an experimental methodology is proposed for the assessment of these technical parameters, based on two lab flume experiments. The first experiment involves investigation of the EMV output in the conditions where the sensor is covered with porous sediment (Ivetić et al., 2018a) of varying depth. The second experiment is focused on describing the distribution of the longitudinal velocity within the lab flume, or more accurately within the CV of the EMV device. The aim of the analysis is to support the simplified framework for the application of the discharge assessment (transiting) procedure, with bed-mounted EMV devices.

The paper has been structured in the following manner: firstly, in the material and methods section, the brief overview of the EMV theory is presented, supplemented by the summary of the bed mounted flat EMV characteristics and the simplified mathematical model of an EMV operating principle. Afterward, the details of the used experimental setup are presented. Material and methods section is closed with the concept of the proposed procedure for the assessment and validation of the (missing) technical parameters. In the next section, the results of the applied procedure, on the used flat bed-mounted EMV, are presented and the derived technical parameters are validated. Finally, in the conclusions, implications of the presented investigation are discussed and the directions for future research are defined.

MATERIAL AND METHODS

2. 1. Mean velocity measurement with the EMV meter

Bed-mounted EMV meters are not commonly used for flow measurements in UDS or in open channel flows. The operating principle of these devices along with the overview of the used EMV characteristics are presented in Ivetić et al. (2018a), while the basics are recapitulated here. Afterward, the simplified mathematical model of an EMV sensor is proposed and the importance of the missing technical parameters is highlighted in the scope of the accurate mean flow velocity assessment.

2.1.1. Basics of the EM velocity sensing theory

EMV operating principle is based on the Faraday's law of induction, where the meter's output signal (induced voltage between the electrodes E) is generated by the motion of the conductive fluid through a transversal magnetic field (Shercliff, 1962). By assuming particular electric and magnetic properties of the environment (Michalski et al., 2001), Kolin (1936) has proposed a basic relationship for the EM theory. General sensitivity was described as the cross product of the velocity and the magnetic field at a certain position (Bevir, 1970; Bevir et al., 1981, Watral et al., 2016). Furthermore, the relations used in electrical networks, motivated an idea to describe how each part of the flow field contributes to the total voltage E measured by the EM sensor, through the weighting function w (Shercliff, 1962) or in a more rigorous formulation, through the weighting vector $\vec{W}$ (Bevir, 1970):

$$E = \int_{\tau} (\vec{B} \times \vec{j}) \cdot \vec{V} d\tau = \int_{\tau} \vec{W} \cdot \vec{V} d\tau \cong \int_{\tau} w \cdot \vec{V} d\tau \tag{1}$$

where $\vec{V}$ is the fluid's streamwise velocity field, $\vec{B}$ is the magnetic field (or induction) of EMV's coils, the cross product $\vec{B} \times \vec{j}$ defines Bevir's weighting vector $\vec{W}$, τ represents the CV of the EM sensor (**Fig. 1**) and $\vec{j}$ is the virtual current vector (i.e. the current density set up in the liquid by driving an imaginary unit current between a pair of electrodes).

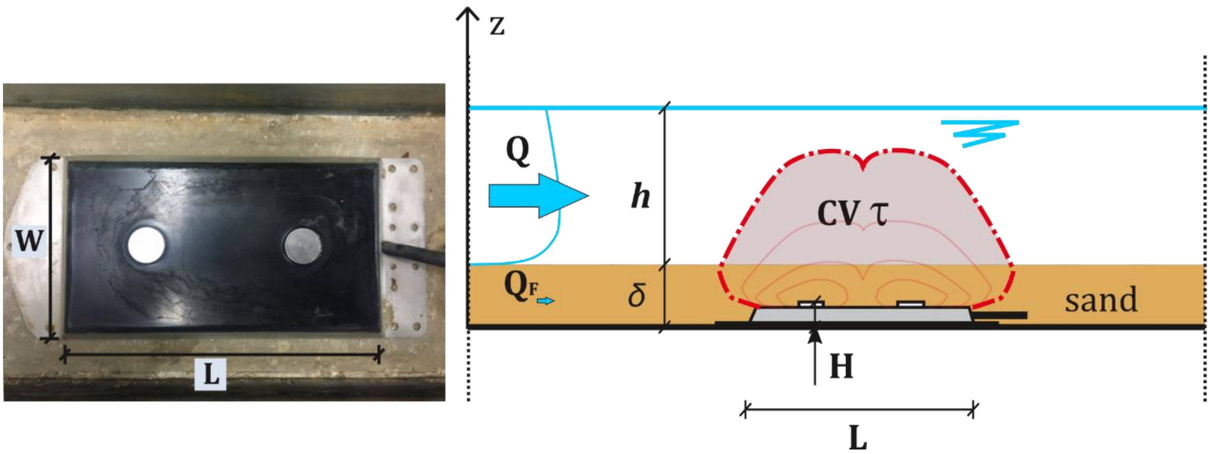

Fig. 1. Left) Flat DC-2 EMV in the lab flume (top view); Right) Illustration of the Flat EMV operation under sand cover with parameters significant to the analysis (longitudinal cross-section)

2.1.2. Bed-mounted flat EMV meter

In the research presented here, bed mounted Flat (coil) DC-2 EMV sensor was used. It is designed by a local SME (Svet instrumenata, 2018) for one-dimensional velocity measurements. The sensors are installed and are continuously operating in the several UDS applications, either on the bottom or on the wall (when multiple sensors are used, e.g. as in Ivetić et al., 2017). For minor conduits, smaller Compact Flat DC-2 EMV is used.

The flat EMV sensor is shaped to minimize the flow disturbances. The used EMV has two flat excitation coils integrated into the robust inox housing, covered with epoxy resin, with the dimensions of L = 280 mm, W = 160 mm and H = 23 mm (**Fig. 1 Left**). The high internal resistance (order of 20 MΩ) reduces the effects of fluid conductivity variations on the velocity measurements. The sensor is connected to external data logger and power source. Data can be collected either wirelessly via GPRS or with the standard RS-232/RS-485 serial interface. The overall cost of one flat DC-2 EMV unit is below 5000 $, being in a similar price range as the one-dimensional non-profiling ADV. Factory calibration of each EMV meter is performed in a towing tank simulating nearly homogenous velocity profile in the CV of the sensor (ISO3455, 2007). The manufacturer specifies that the accuracy of the DC-2 EMV device is $\pm 1\%$ of the measured velocity and the precision 0.001 m/s. The operating range is bidirectional, defined as $\pm$ 15 m/s. Results of the laboratory benchmarking of the measurement uncertainty were reported in Ivetić et al. (2018a). The induced voltage shows a linear relationship with the measured velocity, even in the case of the low flow depths where some deviations were expected due to the effects of the sensor housing on the velocity distribution. The power consumption is user controllable: larger coil currents and longer measurement periods will increase the needed power but will lead to better signal/noise ratio.

2.1.3. A simplified mathematical model of an EMV and (missing) technical parameters

The main source of the flow measurement uncertainty in the VA method is emanating from the mean velocity assessment. A number of investigations involving the usage of bed-mounted ADVs (Hughes et al., 1996; Larrarte et al., 2008), emphasized that the velocity measured V_{meas} is different from the mean flow velocity V, due to the local character of the measurements. Even in sites which satisfy the basic requirements, in terms of the straight sewer reaches with neither deposits nor singularities in the vicinity, a suitable extrapolation is needed to obtain the mean velocity over the entire wet cross section (El Bahlouli & Larrarte, 2018) for the expected range of flows. As EMVs are also measuring the velocity in the local, fixed volume CV, the same conclusions can be drawn. The relationship, or the extrapolation, connecting the measured velocity V_{meas} with the actual mean velocity V, is a function of both the technical parameters of the velocity sensor (describing the size of the CV and the principle of the velocity integration within) and the local hydrodynamic properties (velocity profile) in given flow range.

Equation (1) is used to describe the output of the EM sensors: the output voltage is proportional to the product of the velocity field and the weighting vector $\vec{W}$, or function w, integrated across τ. Due to the complexity of this model, where the output is defined with a volume integral of three vector fields, an attempt is made here to derive the simplified mathematical model of bed-mounted EMVs. The goal of the simplification is to allow the user to easily describe the EMV's operating principle. The simplified model and the appropriate technical parameters of the particular EMV sensor, allow the user to perform discharge assessment (or transiting in El Bahlouli & Larrarte, 2018), in specified geometric configuration of a conduit, for the expected range of flow rates (Ivetić et al, 2018b).

The Faraday's law of induction is governed by the right-hand rule, therefore the main longitudinal velocity component V_x is also the dominant contributor to the output signal. It is deemed that for describing the EMV output, the formulation given by Shercliff (1962), involving the usage of the weighting function w, can be used instead of the vector $\vec{W}$. Thus, it can be concluded that for the modelling of the EMV output, apart from the V_x, it is sufficient to define only the weighting function w and the size of the EMV's CV, the τ.

In general, the CV of a bed-mounted EMV sensor depends on the type of used coils to create the electromagnetic field and can be spatially described as a volume τ (**Fig.1**). Assuming that the longitudinal velocity distribution V_x, across the width and the length of the CV, is not varying significantly, volume integral from eq. (1) can be simplified to one dimension, i.e. the definite line integral. Thus, the integration is performed along a line perpendicular to the surface of the electrodes. It should be noted that, by adopting this simplification, only the effects of velocity profile irregularities across the z direction (perpendicular to the EMV electrodes or across the height of the EMV CV) can be analyzed. Also, by proceeding in this manner, the weighting function w is reduced to one dimensional function $w(z)$. As it will be later shown, in such a case it is reasonable to describe CV by using a single parameter τ_{max}, hereby named as a control volume reach. The reach of the CV τ_{max}, defines the distance between the minimum lower and maximum upper limit of the linear integration (**Fig. 2**). Lower limit of integration is in general defined by the vertical position of the surface of the EMV electrodes Z_{surf}, although in case of the presence of sediment cover of depth δ it should be defined as:

$$Z_L = max\{Z_{surf}, \delta\} \quad (2)$$

As the flow depth h can be lower than the $Z_{surf} + \tau_{max}$, the upper limit of the integration is defined in the following manner:

$$Z_U = min\{Z_{surf} + \tau_{max}, h\} \quad (3)$$

Between these limits, a product of the longitudinal velocity profile and the corresponding one-dimensional weighting function is integrated, hence a measured output V_{meas} can be simulated using the following simplified equation:

$$V_{meas} \cong V_{S,meas} = \int_{Z_L}^{Z_U} w(z) \cdot V_x(z) dz \quad (4)$$

where $V_{S,meas}$ is the simulated EMV output while z is the distance perpendicular to the surface of the electrodes, measured from the bottom of the conduit (or conduit walls if the EMV is mounted on the wall). It should be highlighted that by varying the lower and upper limit of integration, different parts of the $w(z)$ are included in the integral, although the spatial distribution of $w(z)$ remains constant.

The Eqs. (2-4) define the simplified mathematical model of a bed-mounted EMV. In general, different designs of the bed-mounted EMV's are available, with various excitation coil shapes and electrode size and position. However, typically the CV is positioned above the sensor housing. Thus, it is assumed that the presented model can be applied for the simulation of the output originating from different bed-mounted EMV models, if the assumption regarding the negligible variation of the V_x is applicable. By allowing for the simulation of the sensor output, via the presented model, the discharge assessment for typical UDS geometric configurations can be performed (El Bahlouli & Larrarte, 2018). Unfortunately, the parameters $w(z)$ and τ_{max} of particular EMV models, are typically not provided by the sensor manufacturers. Additionally, to the best of the authors knowledge, corresponding recommendations for their definition are not available in the literature.

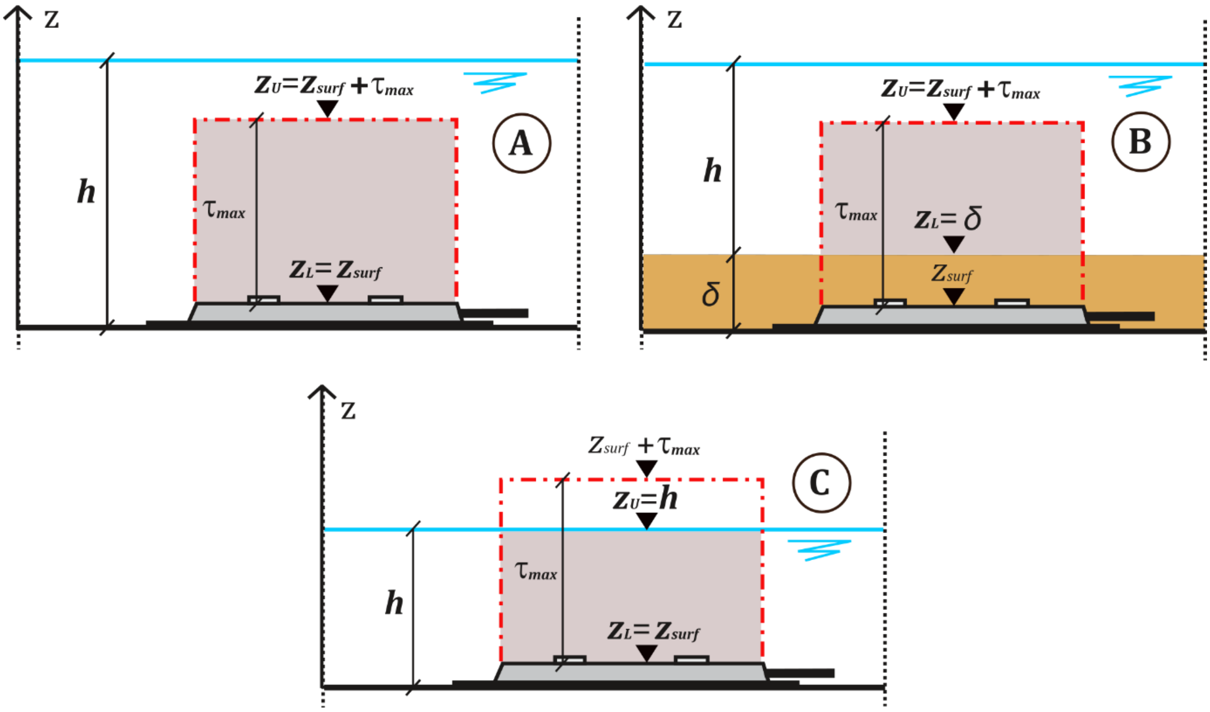

Fig. 2. A simplified mathematical model of a bed-mounted EMV sensor: illustration of the integration limits - A) Standard: Lower limit $Z_L = Z_{surf}$ and the upper limit $Z_U = Z_{surf} + \tau_{max}$, B) Sedimentation: Lower limit $Z_L = \delta$ and the upper limit $Z_U = Z_{surf} + \tau_{max}$, C) Low flow depth: Lower limit $Z_L = Z_{surf}$ and the upper limit $Z_U = h$

2.2. Experimental setup

The lab flume in the Faculty of Civil Engineering, University of Belgrade (Serbia), has been used for the experimental work (Fig. 4 & 5 in Ivetić et al., 2018a). It accommodates the free surface flow in an 8 m long and 0.25 m wide rectangular channel with a controllable downstream flap gate. The flume is connected to the variable frequency drive pump, providing flow rates up to 40 L/s and water depths up to 0.4 m. The whole system can also be controlled with a flow control valve placed at the inlet of the flume. At the inlet pipe, a KROHNE Aquaflux F/6 EMF is mounted with an assessed flow measurement uncertainty of 0.6% for an extended flow range of 2 L/s - 212 L/s. Depth gauge placed perpendicular to the water level and above the EMV meter, covered the range of depths between zero and 40 cm (h_B), with a benchmark uncertainty of 0.2 cm. The EMF and the depth gauge were used for benchmarking the uncertainties of the velocity measurements (Ivetić et al., 2018a), made by Flat EMV placed 4.20 m from the upstream small reservoir and 3.50 m from the downstream flap gate.

Above the flume a traversing system is installed, allowing for the computer-guided servo positioning of the down-looking 3D ADV sensor, for the point velocity measurements. Specifically, the Vectrino PLUS model (Nortek, 2009) was used, with the declared accuracy of 0.5% (in ideal conditions). The ADV was used to measure the velocity distribution within the CV of the EMV. Since the presented system is closed, the conductivity of the water can be considered uniform and constant.

2.3. Assessment of the (missing) technical parameters

The procedure for the assessment of the EMV's one-dimensional weighting function $w(z)$, and the reach of the CV, the τ_{max} is based on the results of two correlated experimental investigations. Firstly, the experiments including the EMV operation under sand sediment of different depths were conducted. It was assumed that the sand sediment is not affecting the EM properties of an EMV sensor (Newman, 1982). In a total of $m = 1 \rightarrow M$ experiments, where $M = 16$, the Flat EMV was covered with the sediment depths of $\delta_m = \{0, 5, 10, 15, 20, 23, 25, 30, 35, 40, 45, 50, 55, 60, 65, 70, 80 \text{ mm}\}$. To prevent the sand from moving, maximum mean flow velocity was kept around 0.30 m/s. The performed experiments were analyzed in Ivetić et al. (2018a). It was concluded that the sediment cover reduced the output signal in a systematic manner. The observed systematic effect on the measurements, can be minimized with the application of the linear regression analysis and resulting linear correction functions, defined by the intercept or zero-shift β and slope or amplification α:

$$\overline{V_{B,m}} = \frac{\overline{V_{EMV,m}} - \beta_m}{\alpha_m} \tag{5}$$

where $\overline{V_{B,m}}$ and $\overline{V_{EMV,m}}$ are benchmark mean velocity and observed velocity, respectively while α_m [-] and β_m [m/s] are the m-th correction function slope and intercept parameter respectively. It was found that the parameters of the correction functions can be modelled if the sediment depth δ is known, therefore a sediment (type) specific Correction Function Model (CFM) was defined and proposed for reduction of the systematic effect of the sediment cover on the velocity measurements.

For the analysis presented here, it is interesting to examine the variation of the correction function parameters α and β against the sediment depth δ. The value of parameter β was found to be constant for varying sediment cover depths. This type of behavior was linked to the fact that the zero shift, β originates from the reduction of the surface of the electrodes due to the presence of the sediment cover (Ivetić et al., 2018a). On the other hand, the value of α, correction function slope or amplification, has shown a clear power like correlation with the sediment depth (**Fig 3**). It was concluded that the observed reduction of the output signal, proportional to δ, was occurring due to the fact that the sediment cover was occupying the lower part of the EMV's CV, hence the Z_L was shifted upwards (Eq. 2 and 4). The parts of the CV occupied with the sediment, where the velocities are negligible ($Q_F \sim 0$, **Fig 1 Right**), were not contributing to the output generation.

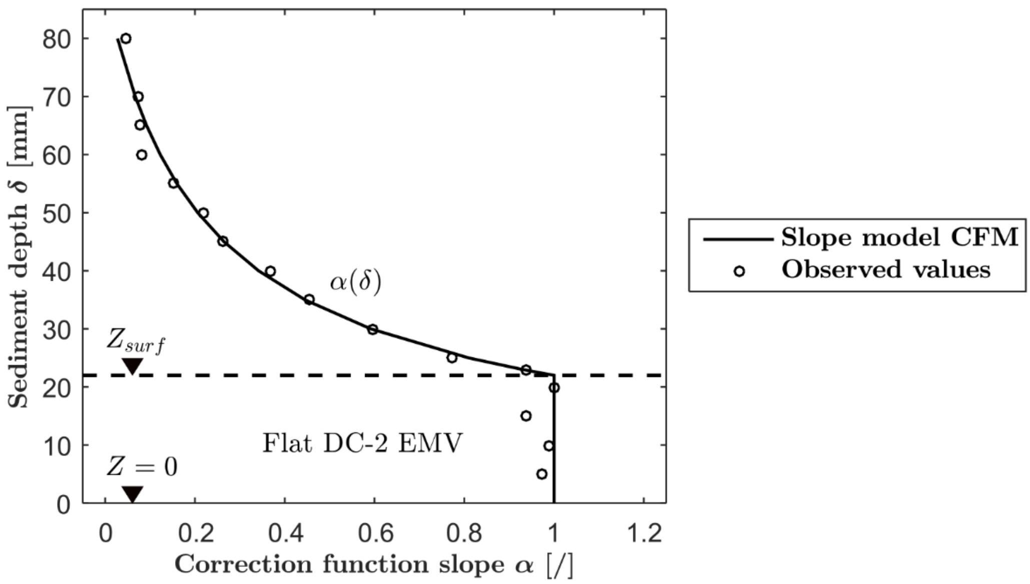

Fig. 3. Correction function slope α values with CFM slope model, obtained after reduction of the bias uncertainty resulting from the presence of the various sand sediment depths $\delta = Z_L$

Further analysis revealed that these results can be used for the derivation of the one-dimensional weighting function $w(z)$ and the reach of the CV, the τ_{max}. The rationale is based on the fact that the sediment cover experiments lead to the correlation between the reduction of the CV size in the direction perpendicular to the electrodes (through $Z_L = \delta$), and the reduction of the EMV output – described through the parameter α. If the actual longitudinal velocity distribution $V_x(z)$ is known, Eq. (4) can be used to assess the missing technical parameters $w(z)$ and τ_{max}. The following subsections are dedicated to the description of the procedures used for the definition of the actual longitudinal velocity distributions in the lab flume through a second experimental investigation, and later the assessment and the validation of the technical parameters.

2.3.1. Assessment of the longitudinal velocity field within the Control Volume

To derive the one-dimensional weighting function $w(z)$, a continuous function describing the longitudinal velocity distribution $V_x(z)$ above the Flat DC-2 EMV was needed to complement the experiments presented in Ivetić et al. (2018a). The experimental analysis of the flat EMV were performed in the lab flume described in the section 2.2. It is important to highlight that during the experiments the aspect ratio Ar (the ratio between the flume width B and channel depth h) was smaller than 5 in most of the cases. Thus, the experiments were performed in the narrow channel setup, where the velocity distribution is three dimensional, and the maximum velocity appears bellow the free surface (Nezu et al., 1986; Bonakdari et al., 2008). The submerged position of the maximum velocity is defined through the value of dip phenomenon, the ξ_{dip}.

In general, for describing the $V_x(z)$ in the fully turbulent channel flow, different formulations are used for the inner and outer regions of the composite turbulent boundary layer. The inner region represents roughly 10-20% of the channel flow depth, and within this region, turbulent kinetic energy generation is dominant over the rate of dissipation. Depending on the wall rugosity, i.e. smooth or rough walls, different formulations can be used for describing the velocity distribution. For the case of rough walls, logarithmic velocity distribution can be used:

$$\frac{V_x}{u_*} = \frac{1}{\kappa} ln\left(\frac{z}{k_s}\right) + B_s \tag{6}$$

where u_* is the shear velocity, κ is the Von-Karman constant, k_s is the roughness height while $B_s = -2.5ln\left(\frac{z_0}{k_s}\right)$. For defining B_s, roughness length of the surface z_0 is needed, which can be determined based on the roughness Reynolds number, using the relations proposed by Jan et al. (2006). Although the porosity of the sand has an influence on the velocity distribution in the inner region, Chen & Chiew (2004) indicated that this relation can be applied for flows over porous beds, if there is no seepage through the bed.

Due to the narrow channel flow setup, analytical velocity distribution that accounts for the dip phenomenon, regarding the value ξ_{dip}, was needed for the outer region. General formulation proposed by Bonakdari et al. (2008) was used here:

$$\frac{V_x(\xi_i)}{u_*} = \left(\frac{\frac{\xi_i^2}{2} + \xi_i + C_{Ar}}{\frac{\xi^2}{2} + \xi + C_{Ar}}\right)\left[\left(\frac{\left(\frac{\xi^2}{4} + \xi + C_{Ar}\ln(\xi)\right) - \left(\frac{\xi_i^2}{4} + \xi_i + C_{Ar}\ln(\xi_i)\right)}{\frac{\xi_i^2}{2} + \xi_i + C_{Ar}}\right) \cdot \frac{\left(\frac{gh\sin\theta}{u_*^2} - 1\right)}{\kappa} + \frac{1}{\kappa} ln\left(\frac{0.2h}{k_s}\right) + B_s\right] \tag{7}$$

where ξ_i is the relative distance from the bottom, ξ is the relative position of the boundary between the inner and outer region, C_{Ar} is the parameter depending on the ξ_{dip} value, while $\sin\theta$ is the energy slope. The expression was derived from the simplified Reynolds Averaged Navier-Stokes equations, taking into the account the previously observed features of the narrow channel flows. The main parameter of this model is defined as $C_{Ar} = 9.3\xi_{dip}^{1.7}$. Several researchers proposed expressions for the value of ξ_{dip}, at the central vertical profile, based on a series of measurements (e.g. Wang et al., 2001; Yang et al., 2004; Bonakdari et al., 2008). To define the most adequate formulation for the ξ_{dip} value, and generally the velocity distribution in the experiments with the Flat EMV, supplementary $V_x(z)$ measurements were performed. Experimental setup described in section 2.2. was used and three cases were analyzed (Table 1.).

Table 1. Flow characteristics of three analyzed cases used for the assessment of the longitudinal velocity distribution within the lab flume

Case	Sediment depth	Flow rate	Flow depth
[/]	[mm]	[L/s]	[cm]

1	20	14.5	20.4
2	25	14.4	20.3
3	0	33.3	32.4

Longitudinal velocity distribution above the Flat EMV was measured within the flume, along three Central Vertical Profiles (CVP). The positions of the CVP 1 and 3 were chosen to be above the EMV's electrodes, while CVP 2 is placed in between (**Fig. 4**). Point velocity measurements were made with the down-looking ADV (Lohrmann et al., 1994). Raw instantaneous velocity measurements were taken using the sampling frequency of 100 Hz and were despiked based on the spike detection algorithm proposed by Goring & Nikora (2002). Despiked measurements were averaged over 30 s interval ($\overline{v_x}$) as suggested by Buffin-Bélanger & Roy (2005).

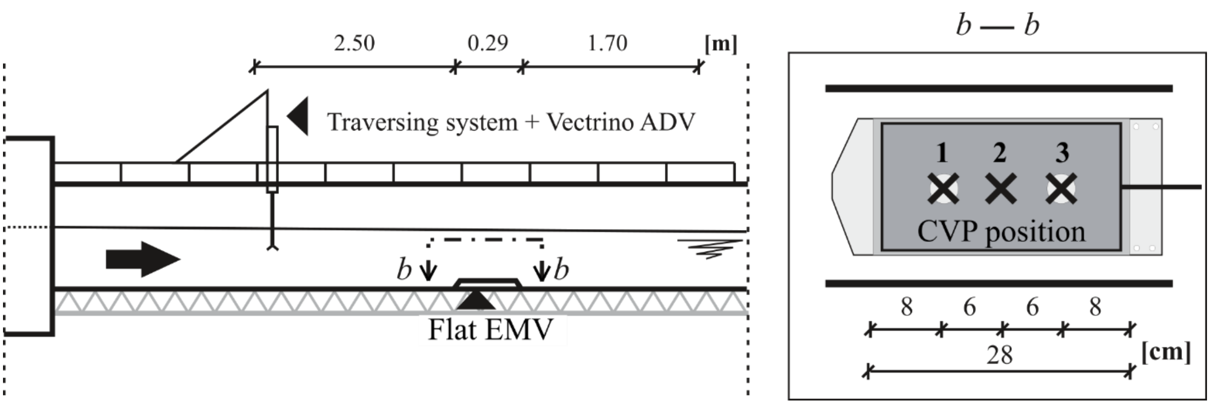

Fig. 4. A schematic illustration of the central vertical profiles (CVP) position above Flat DC-2 EMV used for longitudinal velocity measurement using ADV

2.3.2. Derivation of the technical parameters

The starting point for the derivation of the one-dimensional weighting function $w(z)$ and the reach of the CV τ_{max}, is the simplified mathematical model of the EMV sensor defined with Eqs. (2-4). Following the assumption that the $V_{meas} \cong V_{S,meas}$, the mathematical model shows how V_{meas} can be reduced with the increase of the lower Z_L and reduction of the upper Z_U integration limit. As the magnetic field $\vec{B}$ and virtual current $\vec{j}$ have the highest magnitudes in the vicinity of the electrodes, it is expected that the weighting function $w(z)$ follows a similar distribution. Hence, the increase of the Z_L will have a dominant influence on the V_{meas} reduction (**Fig 2 B**), when compared to the decrease of the Z_U (**Fig 2 C**). Therefore, it can be expected that the correlation between the increase of Z_L and the reduction of V_{meas} is more valuable for the assessment of the technical parameters.

The correlation Z_L-V_{meas} was defined based on the sand sediment experiments reported by Ivetić et al. (2018a). The Z_L was modified in a controllable manner with the sand sediment of various depths δ. The measurements made by the Flat EMV sensor were compared to the ones corresponding to the $Z_L = Z_{surf}$, where the whole weighting function was employed resulting in the $V_{meas} = V_0$ (for V_0, $\alpha = 1$). The **Fig 3** shows that, with the increase of the $Z_L = \delta$ (when $\delta > Z_{surf}$), the V_{meas} has a power like decrease, when compared to the V_0 ($Z_L = Z_{surf}$). If the information regarding the velocity distribution $V_x(z)$ is introduced here, the backward analysis can be used to reveal the actual distribution of the $w(z)$ from Eq. (4). However, the upper limit of integration Z_U (i.e. the reach of the CV) is unknown, thus, the derivation of the missing technical parameters is formulated as a minimization problem, where the set of τ_{max} values are examined to obtain the optimal one.

From the sand sediment experiments (Ivetić et al., 2018a), it was observed that for the maximum sediment depth in the experiments of $\delta = 8.0$ cm, the EMV sensor was producing a small output. This output was generated by the upper parts of the weighting function (with smaller magnitudes), between $Z_L = \delta = 8.0$ cm and unknown Z_U. Thus, the RMSE of the simulated values $V_{S,meas}$ against the measured values V_{meas} observed with sediment depth of $\delta = 8.0$ cm, was deemed as the viable minimization criteria. The minimum examined value of τ_{max} was 6.0 cm, corresponding to the difference between $\delta = 8.0$ cm and Z_{surf}. Also, it was clear that τ_{max} is expected to be similar to this value as the measured velocity for the corresponding sediment depth of $\delta = 8.0$ cm, were around 22 times smaller than the benchmark values (α = 0.045). Therefore, the maximum examined τ_{max} was adopted to be double of the minimum value, i.e. 12.0 cm.

Once the minimization problem was defined, it was necessary to discretize the simplified mathematical model (Eqs. 2 – 4). Since both functions $w(z)$ and $V_x(z)$ are continuous, the definite integral in Eq. (4) can be represented as the sum of products along the vertical line, discretized with an arbitrary Δz. Distance between Z_{surf} and $Z_{surf} + \tau_{max}$ is discretized in N segments, via $i = 0 \rightarrow N$ discretization nodes. For each $\delta_i = Z_{surf} + i\Delta z = Z_{L,i}$, a linear equation in the form of the sum of the products can be used to describe the generation of the output signal $V_{meas,i} = \alpha_i V_0$. The distribution of the $w(z)$ is the characteristic property of the EMV sensor model and is constant in space for varying flow rates, water or sediment depths. On the other hand, for each $Z_{L,i}$ a corresponding velocity distribution $V_x^i(z)$ needs to be defined as with the increase of i the bulk flow is moving further away from the electrodes. Thus, for each $Z_{L,i}$, a different upper segment of the $w(z)$ between $j = i \rightarrow N$ is multiplied with a corresponding $V_x^i(z)$, and integrated to yield $V_{meas,i}$ (**Fig. 5**). In the discretized form this can be represented in the following manner:

$$\alpha_i V_0 = \frac{1}{N}\sum_{j=i}^{N} w_j v_{x,j}^i \tag{8}$$

The Eq. (8) can be interpreted as a discretized version of the simplified mathematical model of an EMV sensor (Eq. 4). For the sake of brevity, a system of N equations (8) can be represented in the matrix form:

$$N\boldsymbol{\alpha}V_0 = \mathbf{wV} \tag{9}$$

where $\boldsymbol{\alpha}$ is the row ($1 \times N$) vector of slope coefficients, $\mathbf{w}$ is the row ($1 \times N$) vector of unknown coefficients of weighting function and $\mathbf{V}$ is the square ($N \times N$) matrix of longitudinal velocity profiles. Due to the fact that the filtration velocity is negligible ($Q_F \sim 0$, **Fig 1 Right**), the matrix $\mathbf{V}$ has a Lower Diagonal (LD) form, where the coefficients above the diagonal, corresponding to the velocities in the sediment cover, are equal to zero. As the derivation of the technical parameters is postulated as a minimization problem, for each examined τ_{max} between 6.0 and 12.0 cm, a corresponding **w** is computed from Eq. (9). Final **w** and τ_{max} are defined based on the min RMSE criterion, between the simulated values $V_{S,meas}$ and observed V_{meas} for the $\delta = 8.0$ cm.

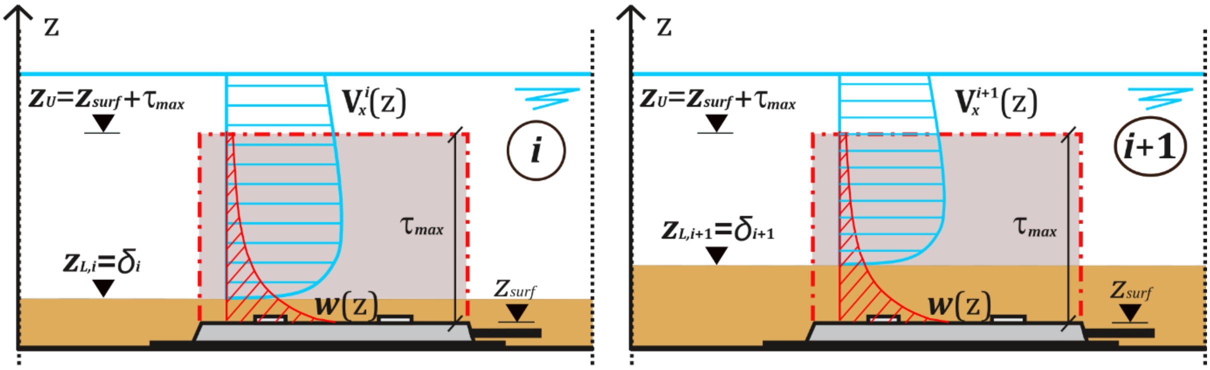

Fig. 5. Schematic illustration of the EMV output signal generation through the interaction between the weighting function $w(z)$ and corresponding velocity distributions $V_x(z)$ for subsequent sediment depths δ_i and δ_{i+1}

2.3.3. Validation of the technical parameters

To validate the proposed simplified mathematical model of the EMV sensor and the derived technical parameters **w** and τ_{max}, an independent set of data measured with the flat EMV was used, extracted from the laboratory tests without sediment cover, reported in the Ivetić et al. (2018a). Within this set, 114 original (unadjusted) velocity measurements were simulated with the proposed model Eqs (2 – 4), and the derived **w** and τ_{max}. Using the results from the assessment of the longitudinal velocity field, specifically from the case 3 (**Table 1**), needed velocity profiles were modelled. Simulated measurements were plotted against the original measurements using the line of perfect agreement (1:1 line) as a reference. The RMSE is reported, conforming to the bias uncertainty (Aguilar et al., 2016), and compared with the adjusted bias uncertainty of the flat EMV sensor (Ivetić et al., 2018a).

RESULTS & DISCUSSION

3.1. Assessment of the longitudinal velocity field within the Control Volume

Following the experimental procedure presented in **2.3.1**, point velocity measurements were made within lab flume, for three different cases (**Table 1.**). Original raw data were despiked using the algorithm proposed by Goring and Nikora (2002) and averaged over 30 s interval. Although several measurements $\overline{v_x}$ were characterized with low SNR values, and therefore could have been rejected, the deviation from the examined velocity profiles were not significant. Overall, the average relative differences for case 1, 2 and 3 were 6.2%, 6.9% and 8.1%. The goal of these experiments was to determine the suitable longitudinal velocity distribution in the lab flume, needed for the derivation of the one-dimensional $w(z)$ (or **w** in discretized form) and the CV reach τ_{max} of the DC-2 Flat EMV sensor.

Longitudinal velocity measurements for the cases 1 and 2, involving the presence of a sediment cover are presented in **Fig. 6** and **7,** respectively. Measurements for case 3, without the sediment, are presented in **Fig. 8**. Due to the geometry of the used lab flume, the effects of the Prandtl's second type of secondary flow resulted in the appearance of the dip phenomenon ξ_{dip}. This effect was captured in all of the measurements, which can be seen on the **Fig. 6 – 8**. To allow for the accurate modelling of such velocity profiles, a theoretical profile in the outer region given by Bonakdari et al. (2008) with several formulations for the location of the ξ_{dip} were examined and compared. It was found that for the examined dispositions, involving rather low aspect ratio Ar values from 0.77 to 1.26, the most suitable fit was observed for the formulation of $\xi_{dip} = 1.3\ \exp(-Ar/2)$, given by Yang et al. (2004). The resulting velocity profiles are shown with a solid line on **Fig. 6 – 8**. However, the velocity measured at the point closest to the bed was found to be 20% higher, in average, than the modelled value. For the cases 1 and 2, this could be attributed to the effect of the porous bed, which was not captured by **Eq. (6)**. On the other hand, for the case 3, the observed deviation could have a different origin, possibly from the housing of the sensor itself. As the observed deviations do not affect the results in a significant manner, it was concluded that the longitudinal velocity profiles in the lab flume can be modelled both in the inner and outer region.

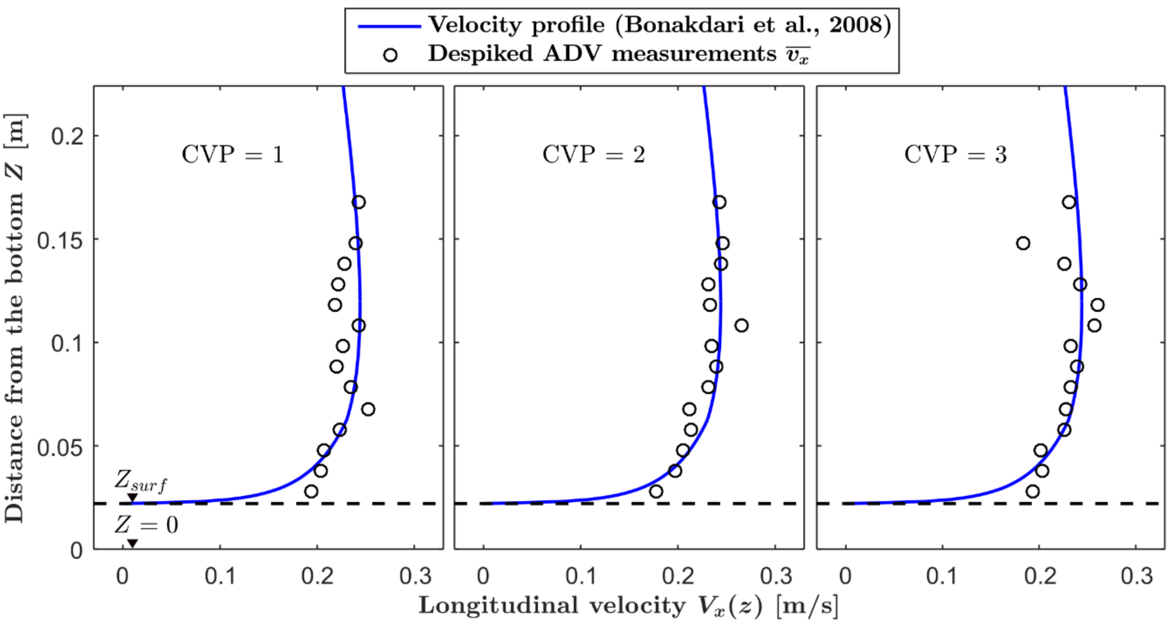

Fig. 6. Despiked longitudinal velocity measurements along three centerlines compared with the logarithmic velocity profile (Bonakdari et al., 2008), for $Q =$ 14.5 L/s, $h = 22.4$ cm, $\delta = 2.0$ cm, $Ar = 1.22$

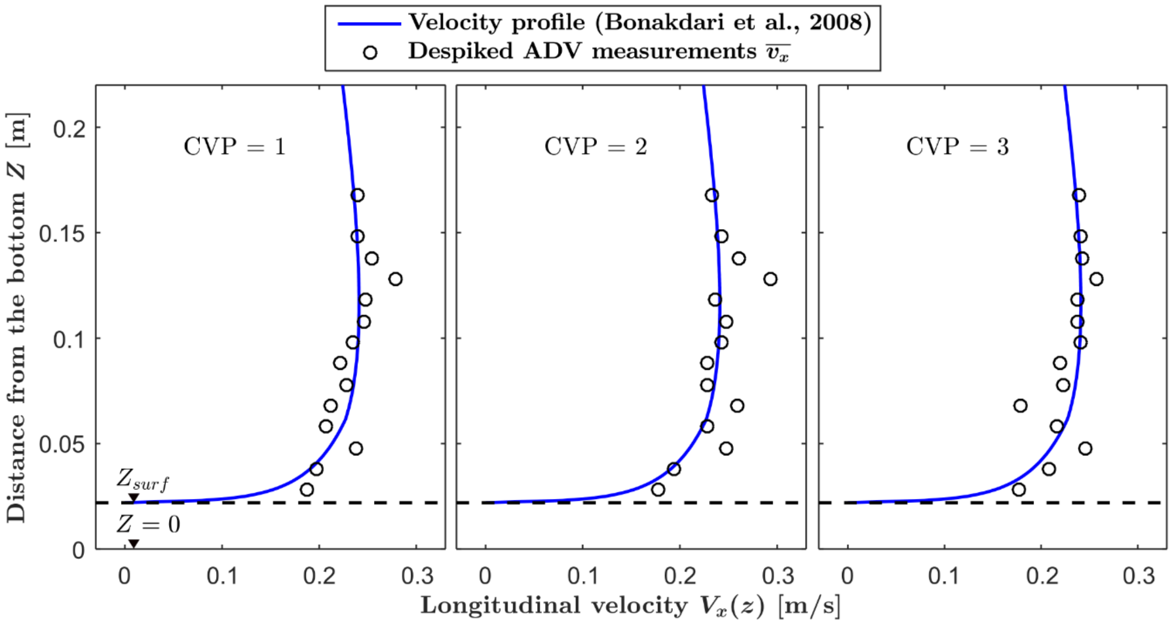

Fig. 7. Despiked longitudinal velocity measurements along three centerlines compared with the logarithmic velocity profile (Bonakdari et al., 2008), for $Q =$ 14.4 L/s, $h = 22.3$ cm, $\delta = 2.5$ cm, $Ar = 1.26$

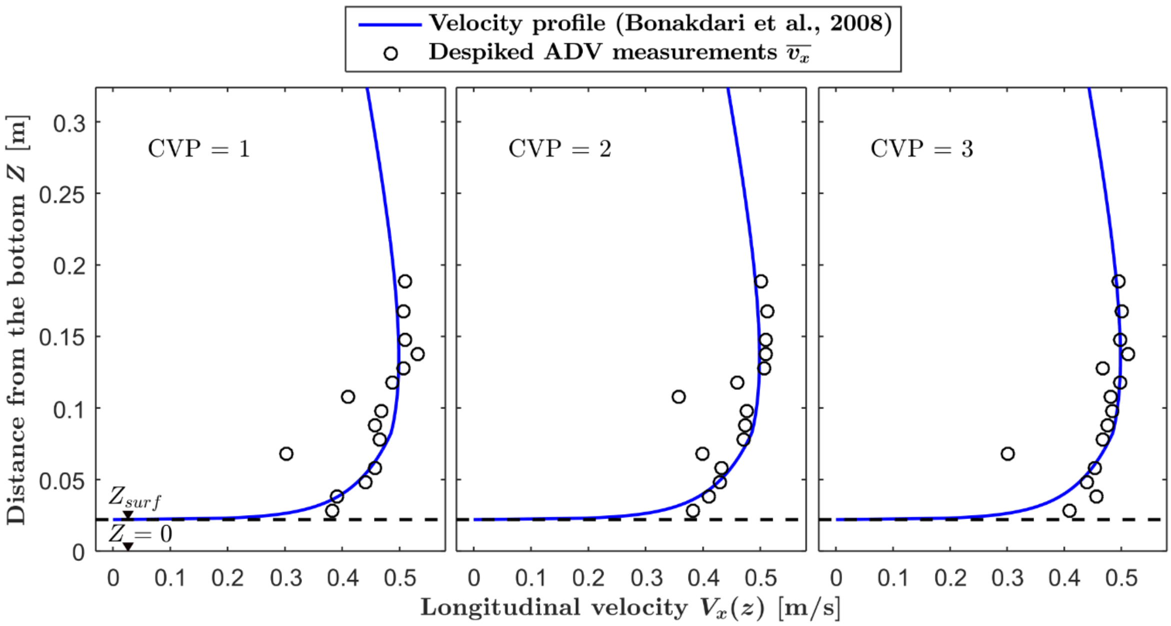

Fig. 8. Despiked longitudinal velocity measurements along three centerlines compared with the logarithmic velocity profile (Bonakdari et al., 2008), for $Q =$ 33.3 L/s, $h = 32.4$ cm, $\delta = 0.0$ cm, $Ar = 0.77$

3.2. Derivation of the technical parameters

Once appropriate theoretical velocity distributions were determined, all of the needed information was available for the formulation of the system of linear equations (**Eq. 8**). The N **Eqs. (8)** form the system of linear equations (**Eq. 9**). As the τ_{max} was not known *a priori*, a set of τ_{max} values were inspected, where for each examined τ_{max} a different system of equations was solved (**Eq. 9**) yielding a set of pairs, computed **w** and τ_{max}. Final value of τ_{max}, and corresponding **w,** were determined by minimizing the RMSE of the simulated values against the unadjusted values observed with the sediment depth of $\delta = 8.0$ cm. It was found that minimal RMSE corresponds to τ_{max} = 8.7 cm, which can be seen on **Fig. 9**. The comparison between the observations simulated with τ_{max} = 8.7 cm and a complementary **w**, and original observations for $\delta = 8.0$ cm, is shown on **Fig. 10**, with a line of perfect agreement (1:1 line) as a reference.

The solution of the system of the linear equations (Eq. 9), for τ_{max} = 8.7 cm, leads to the experimentally defined one-dimensional weighting function **w** (**Fig. 11**). It can be seen that the dominant contribution to the EMV's output is coming from the regions of the CV closest to the electrodes of the sensor. With the increase of the vertical distance from the Z_{surf}, the magnitude of the weighting function w drops, as expected. In the original **Eq. (1)**, the weighting vector or function is defined by the cross product of the magnetic field $\vec{B}$ and virtual current $\vec{j}$. As the distance from the flat coils is increasing, the magnitude of $\vec{B}$ is decreasing. Similarly, the magnitude of $\vec{j}$ is being governed by the magnitude of the $\vec{B}$ and the position of the electrodes, therefore $\vec{j}$ has also the downward trend with the increase of the vertical distance from the sensor electrodes.

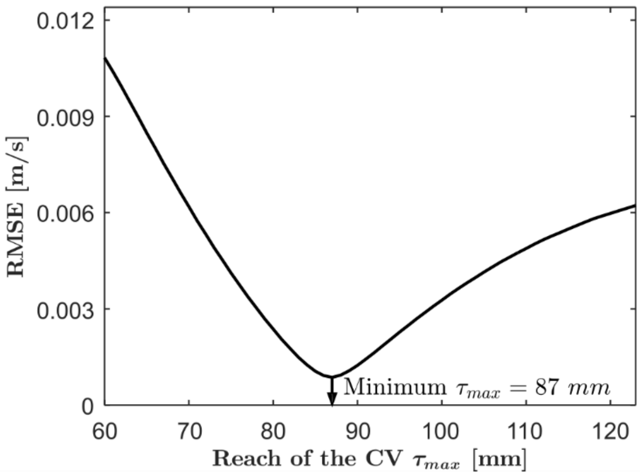

Fig. 9. RMSE between the original and simulated observations made with the DC-2 Flat EMV for the experimental setup with sand sediment depth $\delta = 8.0$ cm, against examined values of reach of the CV τ_{max}

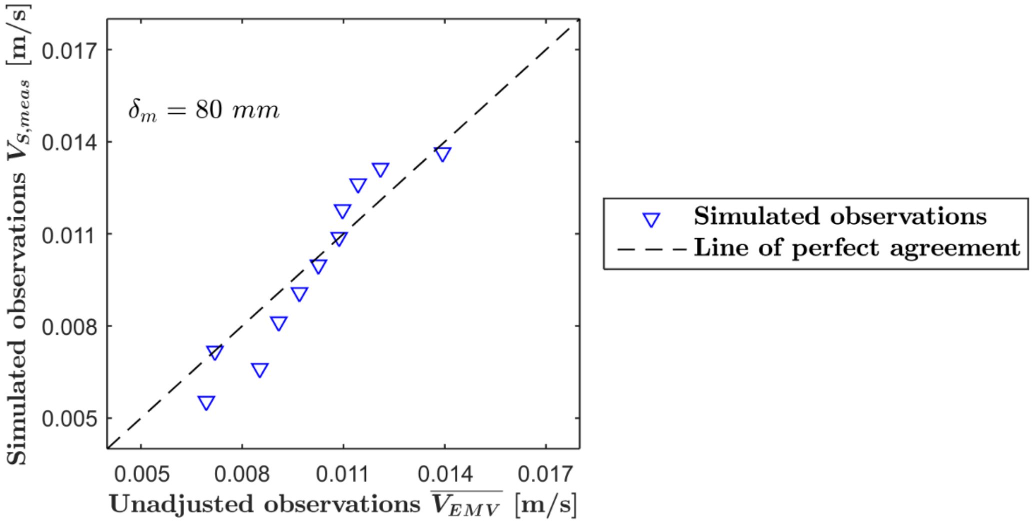

Fig. 10. Observations, simulated with τ_{max} = 8.7 cm, against original unadjusted observations (Ivetić et al., 2018a) made with the DC-2 Flat EMV for the experimental setup with sand sediment depth $\delta =$ 8.0 cm

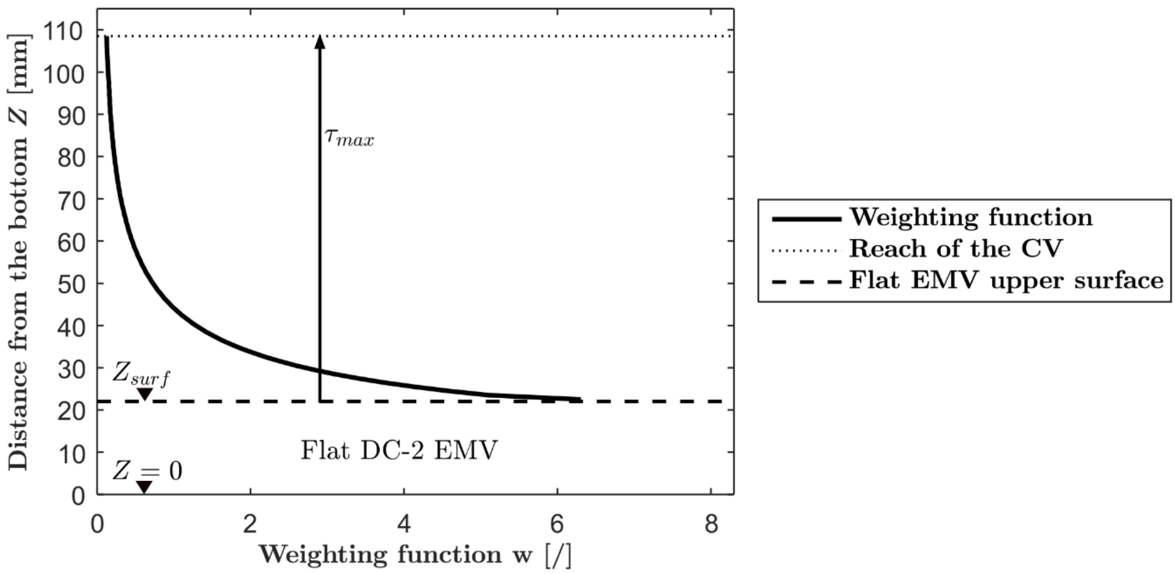

Fig. 11. Experimentally derived one-dimensional weighting function **w** and the reach of the CV τ_{max} for DC-2 Flat EMV, against the distance from the flume bottom ($Z = 0$)

3.3. Validation of the technical parameters

The validation was performed using the set of unadjusted, or original, Flat DC-2 EMV observations reported in the Ivetic et al. (2018a), made on the standard setup without the sediment cover. In section **3.1** it was concluded that the longitudinal velocity distribution in the vertical centerlines can be predicted for different flow conditions, with and without sediment, by using the **Eq. 6 - 7**. For each of the 114 used observations, velocity distribution was modelled and combined with the derived weighting function **w** and τ_{max} to yield the values of the simulated observations $V_{S,meas}$, for given flow conditions. Simulated observation values $V_{S,meas}$ are shown against the original, unadjusted observations $\overline{V_{EMV}}$, with 1:1 reference line of perfect agreement, on **Fig. 12**.

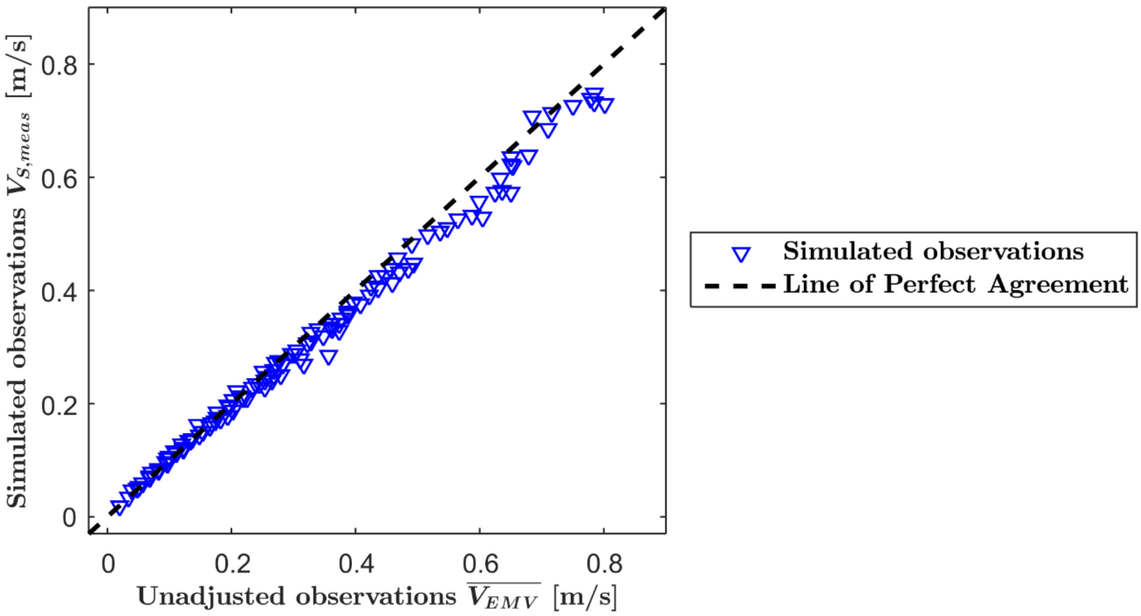

Fig. 12. Simulated observations against original unadjusted observations (Ivetić et al., 2018a) made with the DC-2 Flat EMV for the experimental setup without sand sediment

It can be seen that the simulated observations $V_{S,meas}$ are in decent agreement with the unadjusted observations $\overline{V_{EMV}}$. The computed RMSE value is 0.025 m/s, which is slightly higher than the adjusted bias uncertainty (0.015 m/s) reported in Ivetic et al. (2018a). It is assumed that the higher RMSE value is mainly due to the deviations between the used theoretical velocity distribution and actual velocity distribution. It can be hypothesized that for higher velocities and lower depths, actual longitudinal velocity distribution had higher magnitudes in the inner region.

Based on the presented results, it is concluded that the simplified mathematical model of the EMV sensor can be used to describe the operating principle of these devices in general. Furthermore, it is shown that the missing technical parameters, one-dimensional weighting function **w** and CV reach τ_{max}, can be derived with the proposed experimental methodology for each particular bed-mounted EMV sensor. It should be noted that both **w** and τ_{max} appear to be fixed properties of the examined EMV sensor, as they were applicable to both the cases with and without sand sediment.

CONCLUSIONS

Bed-mounted EMV meters can be considered as a supplement, or an alternative, to commonly used ADVs for flow measurements in UDS. In previous laboratory investigations, it was shown that these devices are more robust and can deliver accurate low flow measurements, even under a porous sediment cover. However, the EMV meters are sampling smaller control volume (CV), which is closer to the sensor than bed-mounted ADV's, in the parts of the flow where velocity gradients are high. Due to the fact that both ADV's and EMV's velocity measurements are deviating from the mean flow velocity, a suitable extrapolation is needed to calculate the flow rate. Extrapolation, covering the range of hydraulic conditions can be defined for specific UDS geometric configuration and the expected range of flow rates. In order to perform this type of analysis, the operating principle of the sensor needs to be modeled.

Fundamentally, the operating principle of the EM devices is described through the volume integral of three vector fields product (magnetic, velocity and virtual current fields). As these vector fields are rarely defined at each specific UDS measurement site, a simplified mathematical model of the EMV meter is suggested here. The suggested model describes the EMV operating principle with only two technical parameters, one-dimensional weighting function w and the reach of the CV, the τ_{max}. It is deemed that the proposed model can be applied to any common bed-mounted EMV sensor application, if it can be assumed that the variation of the longitudinal velocity distribution is negligible across the width and length of the sensor CV.

Furthermore, a novel procedure for the experimental derivation of two technical parameters, w and τ_{max}, is proposed. It is based on two correlated experimental investigations. Firstly, the experiments in which the sensor is covered with porous sediment were used for determining the reduction of the measured velocity due to the variation of the lower integration limit. Secondly, the longitudinal velocity distribution is defined within the integration limits, by combining the theoretical velocity profiles and down-looking ADV measurements. Using the acquired data, the backward analysis is suggested to formulate a minimization problem, from which the unknown technical parameters are assessed.

For the used Flat DC-2 EMV meter the non-linear one-dimensional weighting function was derived. The reach of the CV, for this sensor, defining the maximum upper integration limit, was found to be 8.7 cm. The suggested simplified model of an EMV, and derived technical parameters, were validated against the independent set of data, obtained from previous experiments without sediment (Ivetić et al., 2018a). It was concluded that, if the velocity distribution within the CV reach is known, the velocity measurements can be simulated as the product of the one-dimensional weighting function and longitudinal velocity distribution, integrated between lower and upper integration limits.

The proposed experimental procedure for derivation of w and τ_{max}, is relatively expensive and time-consuming. However, derived technical parameters appear to be invariable properties of the EMV sensor, hence the same set of parameters can be used for different sensor application. When using the suggested model of the EMV for discharge assessment, with experimentally derived technical parameters, longitudinal velocity field within the CV of the sensor needs to be assessed for each examined flow rate. Theoretical velocity distributions can be used if the local hydraulic and geometric properties meet the needed assumptions, otherwise CFD analysis should be applied. Further field investigations, probably supported by CFD analysis, are needed for the assessment of the full practical implications and limitations. The suggested research should lead to the derivation of the robust pre-positioning analysis, needed for the minimization of the associated flow measurement uncertainties in the UDS.

ACKNOWLEDGEMENTS

The authors express the gratitude to the Serbian Ministry of Education and Science for the support through the project TR37010: "Rain water drainage systems as part of the urban and transport infrastructure”.

REFERENCES

Aguilar, M. F., McDonald, W. M., & Dymond, R. L. (2016). Benchmarking laboratory observation uncertainty for in-pipe storm sewer discharge measurements. *Journal of Hydrology*, 534, 73-86.

Bevir, M.K., 1970. The theory of induced voltage electromagnetic flowmeters. *Journal of Fluid Mechanics*, 43(3), 577-590.

Bevir, M.K., O'Sullivan, V.T. and Wyatt, D.G., 1981. Computation of electromagnetic flowmeter characteristics from magnetic field data. *Journal of Physics D: Applied Physics*, 14(3), p.373.

Bonakdari, H. and Zinatizadeh, A.A., 2011. Influence of position and type of Doppler flow meters on flow-rate measurement in sewers using computational fluid dynamic. *Flow Measurement and Instrumentation*, 22(3), 225-234.

Bonakdari, H., Larrarte, F., Lassabatere, L., & Joannis, C. (2008). Turbulent velocity profile in fully-developed open channel flows. *Environmental Fluid Mechanics*, 8(1), 1-17.

Buffin-Bélanger, T. and Roy, A.G., 2005. 1 min in the life of a river: Selecting the optimal record length for the measurement of turbulence in fluvial boundary layers. *Geomorphology*, 68(1-2), 77-94.

Chen, X. and Chiew, Y.M., 2004. Velocity distribution of turbulent open-channel flow with bed suction. *Journal of Hydraulic Engineering*, *130*(2), 140-148.

El Bahlouli, A. and Larrarte, F., 2018. Proposal for improving discharge quantification in urban drainage. *Flow Measurement and Instrumentation*, 60, 51-56.

Godley, A., 2002. Flow measurement in partially filled closed conduits. *Flow Measurement and Instrumentation*, 13(5), 197-201.

Goring, D.G. and Nikora, V.I., 2002. Despiking acoustic Doppler velocimeter data. *Journal of Hydraulic Engineering*, 128(1), 117-126.

Harremoës, P., Capodaglio, A. G., Hellström, B. G., Henze, M., Jensen, K. N., Lynggaard-Jensen, A.,Otterpohl, R. & Søeberg, H. (1993). Wastewater treatment plants under transient loading-Performance, modelling and control. *Water Science and Technology*, 27(12), 71.

Hughes, A.W., Longair, I.M., Ashley, R.M. and Kirby, K., 1996. Using an array of ultrasonic velocity transducers to improve the accuracy of large sewer mean velocity measurements. *Water Science and Technology*, 33(1), 1-12.

ISO3455, 2007. Calibration of rotating-element current-meters in straight open tanks, International Organization for Standardization.

Ivetić, D., Prodanović, D. and Stojadinović, L., and Cvitkovac M. 2017. Improvement of the flow measuring methodology with the flat electromagnetic velocity probes (in Serbian). Original title: Unapređenje metodologije merenja protoka pomoću ravnih elektromagnetnih senzora brzine. *Vodoprivreda*, 49/1-3(285-287), 93-102.

Ivetić, D., Prodanović, D., and Stojadinović, L., 2018a. Bed-mounted Electro Magnetic meters: Implications for robust velocity measurement in Urban Drainage systems. *Journal of Hydrology*, 566, 455-469.

Ivetić, D., Prodanović, D. and Cvitkovac M. 2018b. Water flow measurements in tunnels with combined flow conditions: case study tunnel Dabarsko polje – Fatniĉko polje (in Serbian). Original title: Merenje protoka vode u tunelima pri kombinovanim uslovima tečenja: primer tunela Dabarsko polje – Fatničko polje. *Vodoprivreda*, 50/4-6(294-296), 229-244.

Jan, C.D., Wang, J.S. and Chen, T.H., 2006. Discussion of “Simulation of Flow and Mass Dispersion in Meandering Channels” by Jennifer G. Duan. *Journal of Hydraulic Engineering*, 132(3), 339-341.

Kolin, A., 1936. An electromagnetic flowmeter. Principle of the method and its application to bloodflow measurements. *Proceedings of the Society for Experimental Biology and Medicine*, 35(1), 53-56.

Larrarte, F., 2006. Velocity fields within sewers: An experimental study. *Flow measurement and instrumentation*, 17(5), 282-290.

Larrarte, F., Bardiaux, J. B., Battaglia, P., & Joannis, C. (2008). Acoustic Doppler flow-meters: A proposal to characterize their technical parameters. *Flow Measurement and Instrumentation*, 19(5), 261-267.

Lohrmann, A., Cabrera, R. and Kraus, N.C., 1994, August. Acoustic-Doppler velocimeter (ADV) for laboratory use. In *Fundamentals and advancements in hydraulic measurements and experimentation* (pp. 351-365). ASCE.

Maheepala, U.K., Takyi, A.K. and Perera, B.J.C., 2001. Hydrological data monitoring for urban stormwater drainage systems. *Journal of Hydrology*, 245(1-4), 32-47.

McIntyre, N. and Marshall, M., 2008, August. Field verification of bed-mounted ADV meters. In *Proceedings of the Institution of Civil Engineers-Water Management* (Vol. 161, No. 4, 199-206). ICE Publishing.

Michalski, A., Starzynski, J. and Wincenciak, S., 2001. Electromagnetic flowmeters for open channels: two-dimensional approach to design procedures. *IEEE sensors journal*, 1(1), 52-61.

Nezu, I. and Rodi, W., 1986. Open-channel flow measurements with a laser Doppler anemometer. *Journal of Hydraulic Engineering*, 112(5), 335-355.

Newman, J.D., 1983. Advances in gauging open channels and rivers using ultrasonic and electromagnetic methods. In *International Symposium on Hydrometeorology* June 13-17, 1982, Denver, Colorado. American Water Resources Association, 1983. 15-26.

Nortek, A.S., 2009. Vectrino velocimeter user guide. Nortek AS, Vangkroken, Norway, 621.

Shercliff, J. A. (1962). The theory of electromagnetic flow-measurement. CUP Archive.

Svet instrumenata, 2018. Flat DC2.34 EMV. Product Datasheet (In Serbian). Retrieved from < http://www.si.co.rs/>.

Wang, X., Wang, Z.Y., Yu, M. and Li, D., 2001. Velocity profile of sediment suspensions and comparison of log-law and wake-law. *Journal of Hydraulic Research*, 39(2), 211-217.

Watral, Z., Jakubowski, J. and Michalski, A., 2015. Electromagnetic flow meters for open channels: Current state and development prospects. Flow measurement and Instrumentation, 42, 16-25.

Yang, S.Q. and McCorquodale, J.A., 2004. Determination of boundary shear stress and Reynolds shear stress in smooth rectangular channel flows. *Journal of hydraulic engineering*, 130(5), 458-462.